NASA
Technical Memorandum 88945

USAAVSCOM
Technical Report 86-C-30

Measurements of the Unsteady Flow Field Within the Stator Row of a Transonic Axial-Flow Fan

I—Measurement and Analysis Technique

K.L. Suder
Lewis Research Center
Cleveland, Ohio

M.D. Hathaway
Propulsion Directorate
U.S. Army Aviation Research and Technology Activity—AVSCOM
Lewis Research Center
Cleveland, Ohio

T.H. Okiishi
Iowa State University
Ames, Iowa

A.J. Strazisar and J.J. Adamczyk
Lewis Research Center
Cleveland, Ohio

Prepared for the
32nd International Gas Turbine Conference and Exhibition
sponsored by the American Society of Mechanical Engineers
Anaheim, California, May 31—June 4, 1987

MEASUREMENTS OF THE UNSTEADY FLOW FIELD WITHIN THE STATOR ROW OF A TRANSONIC AXIAL-FLOW FAN
I - Measurement and Analysis Technique

K.L. Suder
National Aeronautics and Space Administration
Lewis Research Center
Cleveland, Ohio 44135

M.D. Hathaway
Propulsion Directorate
U.S. Army Aviation Research and Technology Activity - AVSCOM
Lewis Research Center
Cleveland, Ohio 44135

T.H. Okiishi
Iowa State University
Ames, Iowa 50010

A.J. Strazisar and J.J. Adamczyk
National Aeronautics and Space Administration
Lewis Research Center
Cleveland, Ohio 44135

ABSTRACT

This two-part paper presents detailed laser anemometer measurements of the unsteady velocity field within the stator row of a transonic axial-flow fan. The objective of this study was to provide additional insight into unsteady blade-row interactions within high speed compressors which affect stage efficiency, energy transfer, and other design considerations. Part I of this paper describes the measurement and analysis techniques used for resolving the unsteady flow field features. The ensemble-average and variance of the measured velocities are used to identify the "rotor-wake-generated" and "unresolved" unsteadiness, respectively. The term "rotor-wake-generated" unsteadiness refers to the unsteadiness generated by the rotor wake velocity deficit and the term "unresolved" unsteadiness refers to all remaining contributions to unsteadiness such as vortex shedding, turbulence, mass flow fluctuations, etc. A procedure for calculating auto and cross correlations of the rotor-wake-generated and unresolved unsteady velocity fluctuations is described. These unsteady-velocity correlations have significance since they also result from a decomposition of the Navier-Stokes equations. This decomposition of the Navier-Stokes equations resulting in the velocity correlations used to describe the unsteady velocity field will also be outlined in this paper.

NOMENCLATURE

G	generalized velocity parameter
n	number of measurements or rotor shaft position
N_{RP}	number of surveyed rotor passages
N_S	number of stator blades
PS	pressure surface
R	radial coordinate axis or radial distance (Fig. 5), cm
R'	axis of laser beam bisector (Fig. 5)
$\mathscr{R}$	apparent stress tensor (Eq. 8), $kg/(m/s^2)$
$\mathcal{S}$	estimate of the standard deviation of velocity (from Eq. 2), m/s
SS	suction surface
t	time, s
V	velocity magnitude, m/s
V_{FS}	freestream velocity, m/s
V_T	total absolute velocity = $\sqrt{V_Z^2 + V_\theta^2}$, m/s
$\mathscr{V}$	velocity vector (Eq. 7), m/s
Z	axial coordinate axis, or axial distance (Fig. 5), cm
α	laser beam orientation angle measured from Z axis (Fig. 5), deg
β	laser beam orientation angle measured from θ axis (Fig. 5), deg
γ	laser beam orientation angle measured from R axis (Fig. 5), deg
θ	circumferential coordinate axis, or circumferential distance (Fig. 5), deg
θ'	circumferential coordinate axis perpendicular to beam bisector (Fig. 5)
ρ	density
φ_R	angle between the beam bisector and the radial direction (Fig. 5), deg

φ_Z angle between the fringe normals and the axial direction, (Fig. 5), Deg.

ω rotor angular frequency, s^{-1}

Ω rotor angular position relative to measured stator passage, Deg.

Subscripts

m measured component

z axial component

θ tangential component

1 measured component in direction of first beam orientation angle

2 measured component in direction of second beam orientation angle

Superscripts

$'$ fluctuating component

$\widetilde{\quad}$ ensemble average

$\overline{\quad}$ temporal phase-lock average

$\overline{\overline{\quad}}$ spatial phase-lock average

$\overline{\quad}$ steady-state condition, or time average

AX axisymmetric component

INTRODUCTION

Unsteady interactions are known to affect various aspects of turbomachine performance, including; blade loading (1), stage efficiency (2), heat transfer (3), noise generation (4), and energy transfer (5). In fact, the fundamental mechanism for energy transfer in turbomachines is the unsteady throughflow (6). However, virtually all existing turbomachine design systems are based on the assumption that the flow is steady in time. A better understanding of unsteady flow interactions may, therefore, lead to an improvement in our ability to predict the performance of turbomachines and to corresponding improvements in turbomachinery design practice.

In the past, unsteadiness in turbomachines has been generally categorized as being either "periodic" or "random" ("turbulent"). Flow-field fluctuations resulting from the relative motion between blade rows have been categorized as "periodic" unsteadiness. "Random" unsteadiness has been used as a catch-all term which includes flow-field fluctuations due to turbulence, vortex shedding, global flow-field fluctuations, true random unsteadiness, and any other unsteadiness not correlated with rotor speed. Therefore, in the absence of a more descriptive terminology for unsteady flows typical of turbomachines and to attempt to avoid confusion of terms, we will use the terms "rotor-wake-generated" unsteadiness to describe the unsteadiness generated by the rotor wake velocity deficit, and "unresolved" unsteadiness to refer to the remaining unsteadiness.

In the present experimental investigation, a laser fringe anemometer (LFA) was used to measure the unsteady velocity field within a transonic axial-flow fan stator row. Unlike a hot wire, which provides a continuous sampling of its measureand, an LFA is dependent on the random occurrence of a seed particle crossing the fringe planes of the LFA probe volume. Therefore, due to the discrete sampling characteristic of laser anemometers, a somewhat different approach for analysis and interpretation of laser anemometer results is required.

Part I of this paper describes the measurement and analysis procedures required to obtain information about the unsteady flow field within turbomachines from laser fringe anemometer results. The ensemble-average and variance of the measured velocities are used to identify the "rotor-wake-generated" and "unresolved" unsteadiness, respectively. A procedure for calculating auto and cross correlations of the rotor-wake-generated and unresolved unsteady velocity fluctuations is described and the mathematical significance of these unsteady velocity correlations, which were derived from the Navier-Stokes equations, is outlined. Some limitations of the present application of laser fringe anemometry to the measurement of unsteady flows are discussed.

Part II of this paper describes the application of these techniques to the study of blade row interactions in a single stage transonic axial-flow fan stage. Mean flow-field results as well as "rotor-wake-generated" and "unresolved" unsteadiness results are presented for both a stator with a double circular arc blade shape and a stator which employs a controlled-diffusion blade shape.

LASER MEASUREMENT TECHNIQUE

The laser anemometer system used in the present experimental investigation is a single channel, dual beam, fringe anemometer with on-axis back-scatter collection optics. The system has been previously described in detail (7). The laser fringe anemometer (LFA) is used to obtain information about the ensemble-mean velocity and ensemble-variance of the velocity fluctuations in any desired direction within a plane perpendicular to the laser beam optical path. In the present work, the optical path direction is the radial direction. Therefore, The present LFA system provides no information on the spanwise ensemble-mean velocity or its fluctuations.

Optical access to the research fan flow field is provided through a 3 mm thick glass window which closely conforms to the tip flow path contour in both the circumferential and streamwise directions. The window allows clear optical access to the flow field from about the rotor trailing edge to 150 percent stator axial chord across slightly more than a stator pitch. Fluorescent liquid seed particles, nominally 1-1.4 μm in diameter, are introduced into the flow field through a 6 mm diameter tube located 35 cm upstream of the rotor. The seeder tube is installed in a radial and circumferential actuator to provide capability for positioning the seeder to optimize the data rate each time the laser probe volume location is changed. The LFA system is mounted outside the test apparatus on a supporting structure which is adjustable in the axial, radial, and circumferential directions of the fan coordinate system in order to position the laser probe volume at the individual measurement locations.

Figure 1 shows the meridional location of the surface of revolution on which the LFA measurements were acquired. The measurement surface was determined from a design code prediction of the "streamline" which passes through the rotor trailing edge at 50 percent span from the shroud. The stator blade-to-blade LFA

measurement locations on the 50 percent span measurement surfaces are shown in Fig. 2 for both stator configurations. These locations are fixed relative to the stator, and thus in the absolute frame.

The flows in turbomachinery are extremely complex and involve many sources of unsteadiness. For example, unsteadiness can be generated by the relative motion between blade rows, vortex shedding, global flow-field fluctuations, and turbulence. The LFA, however, does not allow continuous recording of the instantaneous velocity, V(t), like a hot-wire probe would. Instead, the LFA uses a random sampling technique which is triggered whenever a seed particle crosses the fringe planes of the LFA probe volume. Simultaneously, the angular position of the rotor is also recorded. The LFA, therefore, is a statistical measuring device which is used to extract information about the ensemble-mean velocity and ensemble-variance of velocity fluctuations which are acquired over many thousands of revolutions of the rotor.

At each of the survey points shown in Fig. 2, the LFA system was free to acquire velocity measurements whenever a seed particle crossed the LFA probe volume. This resulted in the random acquisition of many velocity measurements during every rotor revolution. An electronic shaft-angle encoder was used to assign each velocity measurement to the proper angular position of the rotor at which it occurred. The shaft angle encoder provided a measure of the rotor angular position by generating and counting 1100 pulses per rotor revolution relative to a fixed once-per-rev location on the rotor disk. Each time a velocity measurement was acquired, the encoder counter was read in order to determine the angular position of the rotor at which the velocity measurement occurred. However, the velocity measurements do not really occur at discrete encoder pulse positions, but rather occur anywhere within an interval (storage segment) between two adjacent encoder pulse positions. All measurements which occur within a storage segment are assigned to the angular location which corresponds to the center of the segment. This location is termed a rotor shaft position.

At each survey point, approximately 30 000 velocity measurements were acquired for each of two separate laser beam fringe-angle orientations set at ±20° of the locally measured steady-state absolute flow angle. For each fringe-angle orientation, the velocity measurements were acquired for 850 separate angular positions of the rotor (shaft positions) which were evenly distributed at 50 shaft positions per rotor pitch across 17 of the 22 rotor blade passages.

The error in any single LFA measurement is a function of many different parameters including random noise in the photomultiplier tube signal. As a result, it is difficult to make estimates of the total uncertainty in an individual LFA measurement since this noise is generated by background radiation which varies with each measurement. However, based on the number of individual LFA measurements acquired at each rotor shaft position, a statistical measure of the uncertainty in the precision of the estimates of the true ensemble-average and variance of the instantaneous velocities can be determined. Uncertainty intervals representing the 95 percent confidence level of the estimates of precision uncertainty are included for each plotted data point. Table 1 lists the significant sources of bias uncertainty for which estimates of the uncertainty were possible. A fairly comprehensive documentation of the sources of experimental uncertainty in LFA measurements, including methodologies for quantifying them, are provided in Ref. (8).

DATA REDUCTION

As previously mentioned, the LFA acquires velocity measurements over many successive rotor revolutions which results in a distribution of velocity measurements for each of the 850 rotor shaft positions for any survey point. Examples of two such velocity distributions acquired at different rotor shaft positions (one in the "free stream" between adjacent rotor wakes, and one within a rotor wake) are shown in Fig. 3. The striking difference between these two velocity distributions illustrates the inability of the present LFA measuring technique to extract detailed information about any unsteadiness which is not correlated to the fundamental rotor rotational frequency. The double-peaked character of the velocity distribution acquired for flow within the rotor wake is a result of vortex shedding (9). The fluctuation of velocity measurements about the center of each peak is partially a result of turbulence, but also includes all other forms of unsteadiness which are not correlated to the fundamental rotor rotational frequency (e.g., rotor speed drift, inlet massflow fluctuations). Because of the present inability to distinguish the exact content of the various sources of unsteadiness which affect these distributions of velocities, the term "unresolved" unsteadiness will be used herein to refer to all unsteadiness which contributes to the spread in the distribution of velocities (e.g., vortex shedding and turbulence).

The "unresolved" unsteadiness is additional to the "periodic" unsteadiness caused by the relative motion between blade rows. Periodic unsteadiness can be further sub-divided into wake interaction and potential flow interactions. However, due to the large axial spacing between blade rows (85 percent of rotor mid-span axial chord), the periodic unsteadiness resulting from potential flow interactions was assumed to be negligible in this case. Therefore, the term "rotor wake-generated" unsteadiness will be used herein to refer to the periodic unsteadiness occurring as a result of the velocity deficit in the rotor wake and relative motion between blade rows.

"Ensemble-averaging" (10) is required in order to decouple the "rotor-wake-generated" unsteady flow-field features from the "unresolved" unsteadiness. As measurements are acquired during each rotor revolution, the LFA data acquisition system automatically sums the measured particle fringe-crossing frequency and its square for every rotor shaft position. Therefore, the ensemble-average velocity and corresponding variance are readily determined for each rotor shaft position as

$$\tilde{V} = \sum_{i=1}^{n} \frac{V_i}{n} \tag{1}$$

$$\tilde{V'^2} = \frac{\left[\sum_{i=1}^{n} (V_i - \tilde{V})^2\right]}{(n-1)} = \frac{\left(\sum_{i=1}^{n} V_i^2 - n\tilde{V}^2\right)}{(n-1)} = S^2 \tag{2}$$

where the superscript $\sim$ denotes the ensemble average, V_i is the instantaneous velocity measured at a particular rotor shaft position during a given rotor revolution, and n is the number of measurements acquired at that particular rotor shaft position. Since there were typically 30 000 measurements acquired for each measured component, and assuming that these measurements were equally distributed across all 850 measured rotor shaft positions, there would be an aver-

age of $n = 35$ measurements per rotor shaft position. A typical distribution of ensemble-averaged velocities across 6 of the 17 measured rotor blade passages is shown in Fig. 4 for one survey point. Due to computer disk storage limitations, the ensemble-average, ensemble variance, and number of measurements for each of the two measured velocity distributions are the only information typically recorded for each rotor shaft position.

The ensemble-averaged results determined from data acquired at multiple beam orientations were then used to calculate, for every rotor shaft position at each survey point, the ensemble-averaged velocity components in the research fan coordinate system. The research fan coordinate system and LFA beam geometry orientation are shown in Fig. 5. The measured velocity component V_m lies along line AA, which is in the plane of the beams and perpendicular to the bisector of the crossing beams. The beam bisector can be deflected in the off-radial direction, denoted by φ_R, but is restricted to the (R,θ) plane. The direction of the fringe normals can be rotated about the R'-axis (which is aligned with the beam bisector). The angle between the fringe normals and the Z-axis is denoted by φ_Z and is measured in the (Z,θ') plane. For the present investigation the velocity was measured at only two different fringe angle orientations, φ_Z for each φ_R. In addition, $\varphi_R = 0$ for most survey points. Therefore, the ensemble-average velocity components in the research fan coordinate system are related to the measured ensemble-average velocity components through the following two equations.

$$\tilde{V}_Z \cos \alpha_m + \tilde{V}_{\theta'} \cos \beta_m = \tilde{V}_m \qquad (3)$$

where subscript m is assigned the values 1 or 2 corresponding to the two different beam orientations, and

$$\cos \alpha = \cos \varphi_Z$$
$$\cos \beta = \cos \varphi_R \sin \varphi_Z$$

Near the stator surface, although the φ_R angles for the two runs are equal, they are set to some nonzero value in the range -6 to +12° (pressure to suction surface, respectively) in order to reduce beam blockage due to the LFA window frames. Thus, the tangential component of velocity calculated from Eq. (3) actually lies along the θ' direction when $\varphi_R \neq 0$. Although this procedure introduces an additional error source in the measurements (2.2 percent at 12°), it was considered a reasonable sacrifice to obtain some indication of the nature of the flow field close to the stator surface, which would otherwise not be possible to obtain.

Earlier investigations (11) have demonstrated the periodicity of the flow field between the rotor passages of this research fan. Present measurements confirm periodicity. Figure 6(a) shows the superposition of the ensemble-average axial velocity profiles across each of 17 surveyed rotor blade passages for one survey point. Similarly, Fig. 6(b) shows the superposition of the blade-to-blade distributions of the ensemble-average variances across each of the 17 surveyed rotor blade passages. Knowing that periodicity exists, all ensemble-averaged velocity components presented herein are temporally phase-lock averaged as follows:

$$\tilde{\tilde{G}}_j = \frac{\sum_{i=1}^{N_{RP}} G_{j,i}}{N_{RP}} \qquad (4)$$

where G represents any flow-field parameter (ensemble mean or variance), the subscript $j = 1$ to 50 denotes a particular shaft position measured relative to the suction surface of the i'th rotor passage, the superscript $\tilde{\tilde{\ }}$ denotes the temporal phase-lock average, and N_{RP} is the total number of rotor passages surveyed (i.e., 17 passages). The temporal phase-lock averaging operator is applied to the ensemble average variance of the velocities in an attempt to minimize the influence of geometry-induced passage-to-passage flow-field variations (e.g., due to manufacturing tolerances or installation procedures) from artificially increasing the magnitude of the "unresolved" unsteadiness. The successive application of Eq. (4) for each rotor shaft position results in a description of the flow field at 50 equally spaced shaft positions across a representative rotor passage (Fig. 7). The temporal phase-lock average and variance of the axial and tangential velocity components are assumed to characterize the fundamental features of "rotor-wake-generated" and "unresolved" unsteadiness respectively, and are therefore used to determine all other reduced flow-field quantities. Since all results presented herein have been temporally phase-lock averaged, the superscript $\tilde{\tilde{\ }}$ will be dropped hereafter.

Figure 8 shows the relationships between various velocity averages, as well as their relationships with the "rotor-wake-generated" and "unresolved" velocity fluctuations for both continuously sampled hot-wire and randomly sampled LFA measurements. The instantaneous velocity is decomposed into a steady-state velocity $\bar{V}$, a periodic "rotor-wake-generated" fluctuating velocity $\tilde{V}$, and an "unresolved" velocity fluctuation V'. For continuously sampled hot-wire measurements, $\bar{V}$ is the ensemble average of V. For randomly sampled LFA measurements, $\bar{V}$ represents the temporal phase-lock average. The steady-state velocity is determined from arithmetically averaging the distribution of temporally phase-lock averaged velocities across all 50 rotor shaft positions for any survey point, and is used as an estimate of the true time-average velocity. From the above velocity decomposition, and using the temporal phase-lock averages to represent typical rotor passage distributions of ensemble-average parameters, the following velocity correlations can be determined from the LFA measurements.

$$\overline{\tilde{V}_i' \tilde{V}_j'} = \overline{(\tilde{V} - \bar{V})_i (\tilde{V} - \bar{V})_j} \quad ; \quad \text{RWVC} \qquad (5)$$

$$\overline{\tilde{\tilde{V}}_i' \tilde{\tilde{V}}_j'} = \overline{\tilde{\tilde{(V - \tilde{V})}}_i \tilde{\tilde{(V - \tilde{V})}}_j} \quad ; \quad \text{UVC} \qquad (6)$$

where the subscripts i,j correspond to the axial and/or tangential velocity components. $\overline{\tilde{V}_i' \tilde{V}_j'}$ represents the magnitude of the "rotor-wake-generated" unsteadiness (RWVC), and $\overline{\tilde{\tilde{V}}_i' \tilde{\tilde{V}}_j'}$ represents the magnitude of the "unresolved" unsteadiness (UVC).

During the present research program, a single-component laser anemometer system was used to acquire the data. Since the velocity measurements were independently acquired at two different beam orientations, it is not possible to measure cross correlations between the instantaneous measured velocity components. As a result, it is not possible to determine the axial or tangential components of the "unresolved" unsteadiness. However, the following procedure to estimate the

upper and lower bounds of the variances of the velocity components in the axial and tangential directions has been developed.

The LFA data at a given survey point consists of measurements acquired at two different fringe-angle orientations labeled as measurement directions 1 and 2 respectively in Fig. 9. Equations (1) and (2) are used to calculate the variance of the data acquired in each measurement direction. The measured mean velocities $\tilde{V}_1$ and $\tilde{V}_2$ are used to calculate the total absolute mean velocity $\tilde{V}_T$ and the mean flow angle $\tilde{\beta}_T$. The mean and variance are used to define two measurement envelopes, $\tilde{V}_1 \pm \mathcal{J}_1$ and $\tilde{V}_2 \pm \mathcal{J}_2$, which are normal to measurement directions 1 and 2, respectively. The shaded parallelogram shown in Fig. 9 defines the region in the V_Z-V_θ plane which is common to these measurement envelopes. The upper and lower bounds of the variance of the axial and tangential velocity components can therefore be determined by projecting the vertices of this parallelogram onto the V_Z and V_θ axes. Unfortunately these bounds are extremely large, and therefore they provide little useful information. Therefore, the variances of the velocity components which lie in the actual measurement directions, $\mathcal{J}_1$ and $\mathcal{J}_2$ are generally used instead of the axial and tangential component bounds to provide information about the nature of the "unresolved" velocity correlations.

SUMMARY OF AVERAGE-PASSAGE MODEL

Adamczyk (12) has developed a system of equations for simulating the flows in multi-stage turbomachinery which provides a mathematical basis for the aforementioned rotor-wake-generated and unresolved unsteady-velocity correlations (Eqs. (5) and (6), respectively). Adamczyk calls his system of equations the "average passage" form of the Navier-Stokes equations. The average passage system of equations considers a steady-state description of the flow field in an "average passage" of any specific blade row. In a multistage turbomachine, the number of stator blades in successive stages usually differs. Since stator blade wake effects are influential in downstream stator rows, different stator blade numbers in each stator blade row can result in spatially aperiodic flows in downstream stator blade passages. An example of this aperiodicity is shown in Fig. 10. The same is true in general for rotor blade rows. An "average" of the flows in the different blade passages of a specific blade row is the "average passage" flow. The average passage system of equations are ideally suited for use in a turbomachine design system. Unlike current turbomachine design systems, however, the average passage system of equations includes terms which can account for the effects of the unsteady flows. These terms look, in form, much like Reynolds stress terms and identify the major contributors to the generation of nonaxisymmetric flows in multistage turbomachines.

In the derivation of the average-passage system of equations (12), Adamczyk assumed that the absolute velocity field, with respect to a given blade row, could be decomposed as

$$\mathcal{V} = \overline{\overline{\mathcal{V}}} + \overline{\overline{\mathcal{V}}}^{\,\prime} + \tilde{\mathcal{V}}' + \mathcal{V}' \qquad (7)$$

where the first term on the right hand side is the steady-state passage-to-passage averaged component, the second term is the passage-to-passage aperiodic component, the third term is the temporally periodic fluctuating component due to the relative motion between blade rows, and the last term is the component due to unresolved velocity fluctuations (Fig. 10). The passage-to-passage averaged component describes a steady-state flow field which is the same in each blade-to-blade passage of a blade row. The passage-to-passage aperiodic component arises from differing rotor (stator) blade counts in successive stages. In a single-stage turbomachine the aperiodic component would be zero. It should be noted that all averages in the above equation are density weighted averages, according to Adamczyk's derivation. Adamczyk then substituted the above velocity decomposition into the Navier-Stokes equations and, in a manner analogous to Reynolds averaging the Navier-Stokes equations, performed the following averages:

(1) An ensemble average to decouple the periodically unsteady flow-field features from the unresolved unsteadiness.

(2) A time average to decouple the steady-state flow-field features from the temporally periodic unsteadiness.

(3) A phase-lock average to decouple the passage-to-passage average flow-field features from the passage-to-passage aperiodic flow-field features.

As a result, the average-passage system of equations was developed. From the derivation of the average-passage system of equations, the following 2nd-order tensor was identified.

$$\mathcal{R}_{ij} = -\overline{\overline{\rho}}\,\overline{\overline{\tilde{V}_i'\tilde{V}_j'}} - \overline{\overline{\rho}}\,\overline{\overline{\tilde{V}}_i'\tilde{V}_j'} - \overline{\overline{\rho V_i'V_j'}} \qquad (8)$$

where subscripts i and j are tensor indices which correspond to the axial, tangential, or radial velocity components. The variable ρ is the fluid density, and $\mathcal{R}$ is the total apparent stress. The first term on the right-hand side of the equation is the stress due to passage-to-passage aperiodicity, the second term is the stress due to periodic unsteadiness, and the last term is the stress due to unresolved unsteadiness. This total apparent-stress tensor is generic to the average-passage system of equations, and along with body forces and energy terms, its evaluation constitutes the closure problem for this equation system.

Since the data presented herein were acquired in only one stator passage of a single-stage fan, there is no stator passage-to-passage aperiodicity. Therefore, the aperiodic stress term of Eq. (8) equals zero. In addition, although the measured flow field is compressible, there was no means of measuring the time-resolved density, therefore, Eq. (8) cannot be identically calculated from the presently measured data. However, if the density fluctuations are negligible compared to the velocity fluctuations, we can rewrite Eq. (8) as

$$\mathcal{R}_{ij} = -\overline{\overline{\rho}}\left(\overline{\tilde{V}_i'\tilde{V}_j'} + \overline{\tilde{V}_i'V_j'}\right) \qquad (9)$$

The terms $\overline{\tilde{V}_i'\tilde{V}_j'}$ and $\overline{\tilde{V}_i'V_j'}$ correspond to the rotor-wake-generated and unresolved unsteady-velocity correlations, respectively, of Eqs. (5) and (6). If appropriate modeling of the above correlations were possible, Adamczyk's average passage model would have the potential to be used to assess how various design parameters influence flow-field performance when unsteady effects are included. The model could therefore be used to evaluate the potential for controlling the effects of unsteady flows.

SUMMARY AND CONCLUSIONS

In Part I of this paper, a procedure for the measurement and analysis of unsteady flows in turbomachines using a laser anemometer has been described. The analysis includes a methodology for identifying "rotor-wake-generated" and "unresolved" unsteadiness, and for determining corresponding unsteady-velocity correlations. A mathematical basis for the rotor-wake-generated and unresolved unsteady-velocity correlations is also summarized. In Part II of this paper, the magnitudes and distributions of the rotor-wake-generated and unresolved unsteady-velocity correlations are presented and discussed for two different stator blade rows operating behind a transonic axial-flow fan. Also presented are the steady-state absolute velocity field measurements and the kinematics of the transport of the rotor wakes through the stator row.

REFERENCES

1. Gallus, H.E., Lambertz, J., and Wallmann, T., "Blade-Row Interaction in an Axial-Flow Subsonic Compressor Stage," Journal of Engineering for Power, Vol. 102, No. 1, Jan. 1980, pp. 169-177.

2. Yurinskiy, V.T., and Shestachenko, I. Ya., "Losses in an Impulse Turbine Cascade in an Unsteady Flow," Fluid Mechanics-Soviet Research, Vol. 3, No. 1, Jan.-Feb. 1974, pp. 22-27.

3. Doorly, D.J., and Oldfield, M.L.G., "Simulation of Wake Passing in a Stationary Turbine Rotor Cascade," Journal of Propulsion and Power, Vol. 1, No. 4, July-Aug. 1985, pp. 316-318.

4. Gallus, H.E., Grollius, H., and Lambertz, J., "The Influence of Blade Number Ratio and Blade Row Spacing on Axial-Flow Compressor Stator Blade Dynamic Load and Stage Sound Pressure Level," Journal of Engineering for Power, Vol. 104, No. 3, July 1982, pp. 633-641.

5. Zierke, W.C. and Okiishi, T.H., "Measurement and Analysis of Total-Pressure Unsteadiness Data from an Axial-Flow Compressor Stage," Journal of Engineering for Power, Vol. 104, No. 2, Apr. 1982, pp. 479-488.

6. Dean, R.C., Jr., "On the Necessity of Unsteady Flow in Fluid Machines," Journal of Basic Engineering, Vol. 81, No. 1, Mar. 1959, pp. 24-28.

7. Powell, J.A., Strazisar, A.J., and Seasholtz, R.G., "Efficient Laser Anemometer for Intra-Rotor Flow Mapping in Turbomachinery," Journal of Engineering for Power, Vol. 103, No. 2, Apr. 1981, pp. 424-429.

8. Patrick, W.P. and Paterson, R.W., "Error Analysis for Benchmark Fluid Dynamic Experiments, Part I: Error Analysis Methodology and the Quantification of Laser Velocimeter Error Sources." United Technologies Research Center, Report No. R85-151772, June 1985.

9. Hathaway, M.D., Gertz, J.B., Epstein, A.H., and Strazisar, A.J., "Rotor Wake Characteristics of a Transonic Axial-Flow Fan," AIAA Journal, Vol. 24, No. 11, Nov. 1986, pp. 1802-1810.

10. Bendat, J.S. and Piersol, A.G., Random Data: Analysis and Measurement Procedures. Wiley-Interscience, New York, 1971.

11. Strazisar, A.J., "Investigation of Flow Phenomena in a Transonic Fan Rotor Using Laser Anemometry," Journal of Engineering for Gas Turbines and Power Vol. 107, No. 2, Apr. 1985) pp. 427-435.

12. Adamczyk, J.J., "Model Equation for Simulating Flows in Multistage Turbomachinery," ASME Paper 85-GT-226, Mar. 1985.

TABLE I. - ESTIMATES OF BIAS UNCERTAINTY IN VELOCITY MEASUREMENTS

Statistical bias, percent:	
Within rotor wakes	1.2
Outside rotor wakes	0.3
Angle bias, percent	
Within rotor wakes	3
Outside rotor wakes	1
Negative velocity bias due to flow reversals	unable to estimate
Bias due to probe volume position uncertainty, percent	0.2

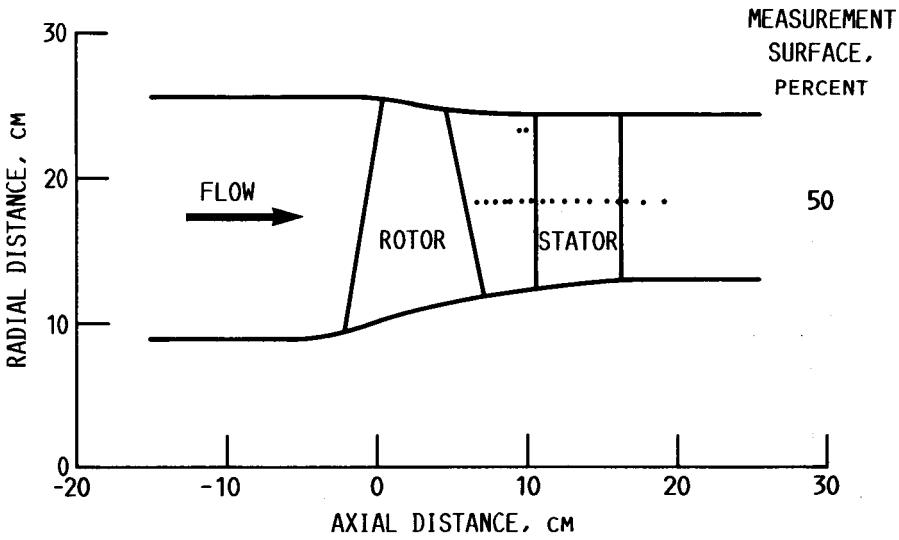

FIGURE 1.- MERIDIONAL-PLANE VIEW OF RESEARCH FAN FLOW PATH SHOWING THE 50 PERCENT SPAN MEASUREMENT SURFACE ALONG WHICH THE LASER ANEMOMETER DATA WERE ACQUIRED.

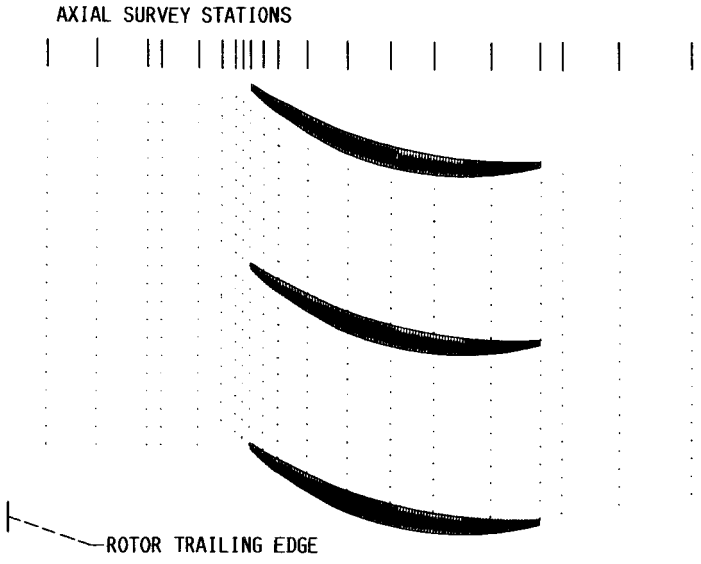

(A) DCA STATOR PASSAGE.

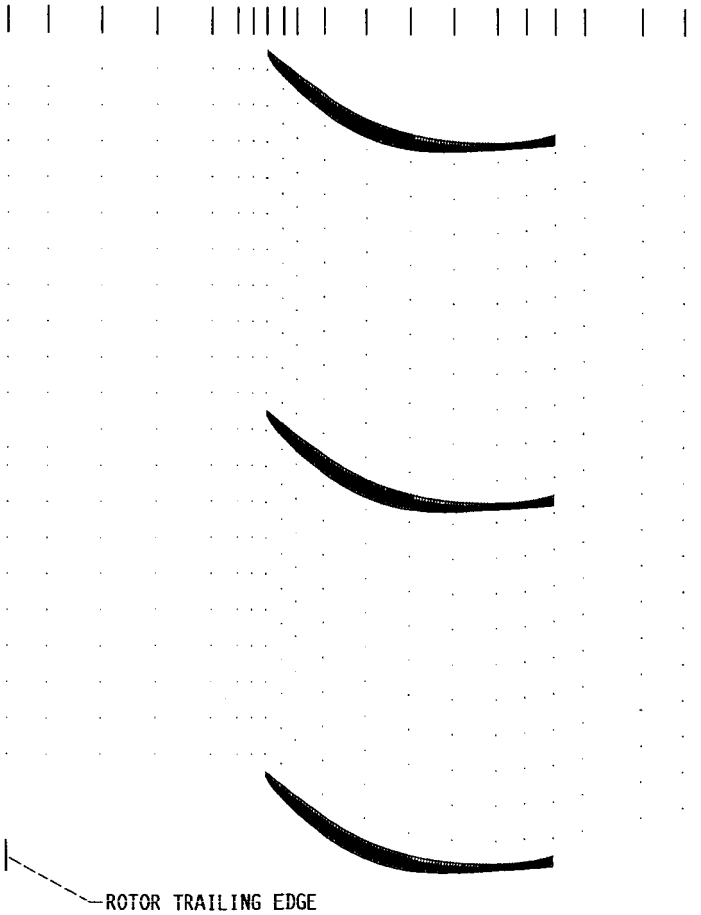

(B) CD STATOR PASSAGE.

FIGURE 2. - BLADE-TO-BLADE VIEW OF THE MIDSPAN SURFACE SHOWING THE LASER ANEMOMETER MEASUREMENT SURVEY POINTS.

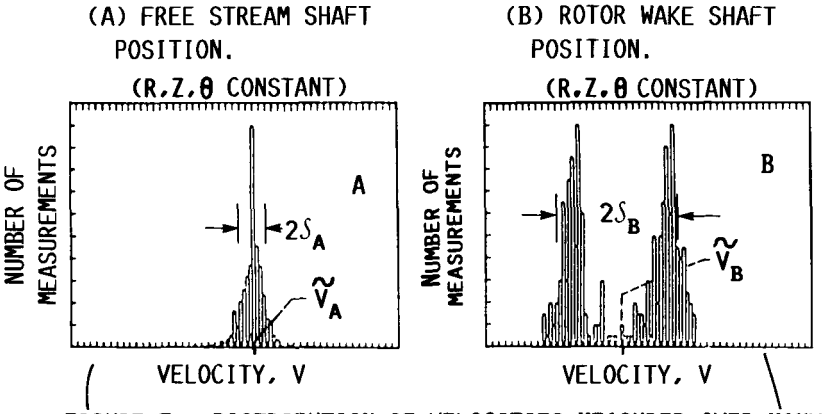

FIGURE 3.- DISTRIBUTION OF VELOCITIES MEASURED OVER MANY SUCCESSIVE ROTOR REVOLUTIONS FOR TWO DIFFERENT ROTOR SHAFT POSITIONS.

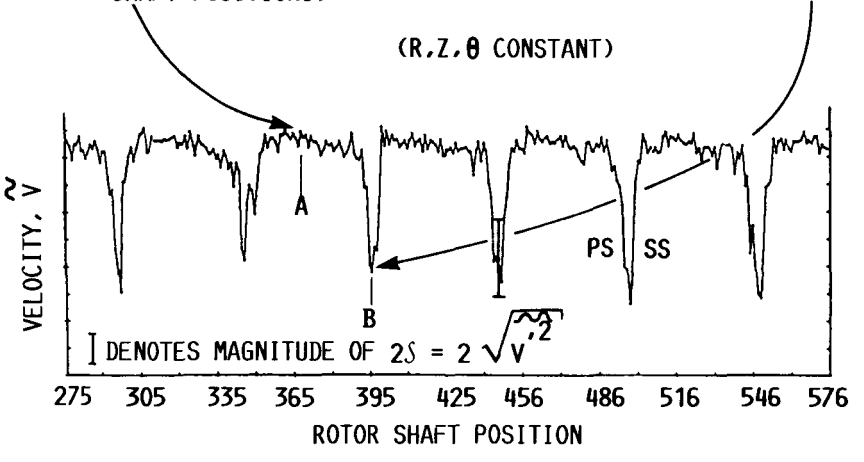

FIGURE 4.- TYPICAL DISTRIBUTION OF ENSEMBLE-AVERAGE VELOCITIES ACROSS 6 OF THE 17 MEASURED ROTOR BLADE PASSAGES.

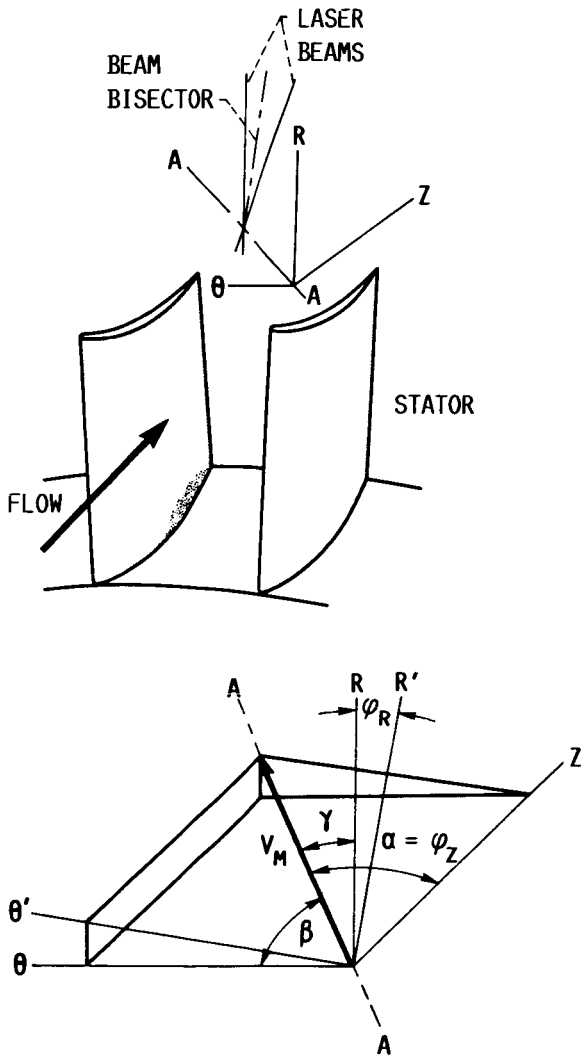

FIGURE 5.- RESEARCH FAN COORDINATE SYSTEM AND LASER BEAM GEOMETRY ORIENTATION.

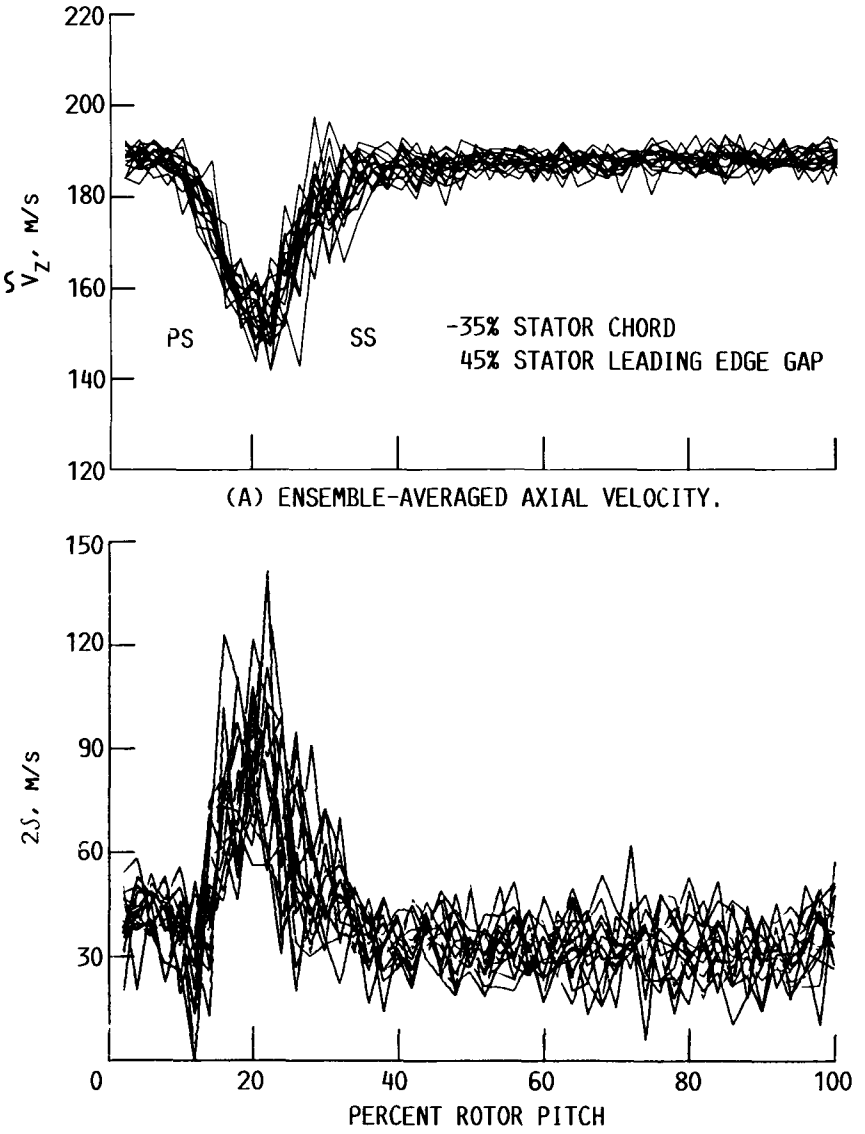

(A) ENSEMBLE-AVERAGED AXIAL VELOCITY.

(B) SQUARE ROOT OF VARIANCE TIMES TWO. (OR x 2).

FIGURE 6.- PERIODICITY OF ENSEMBLE-AVERAGE VELOCITY DISTRIBUTIONS ACROSS EACH OF THE 17 SURVEYED ROTOR PASSAGES.

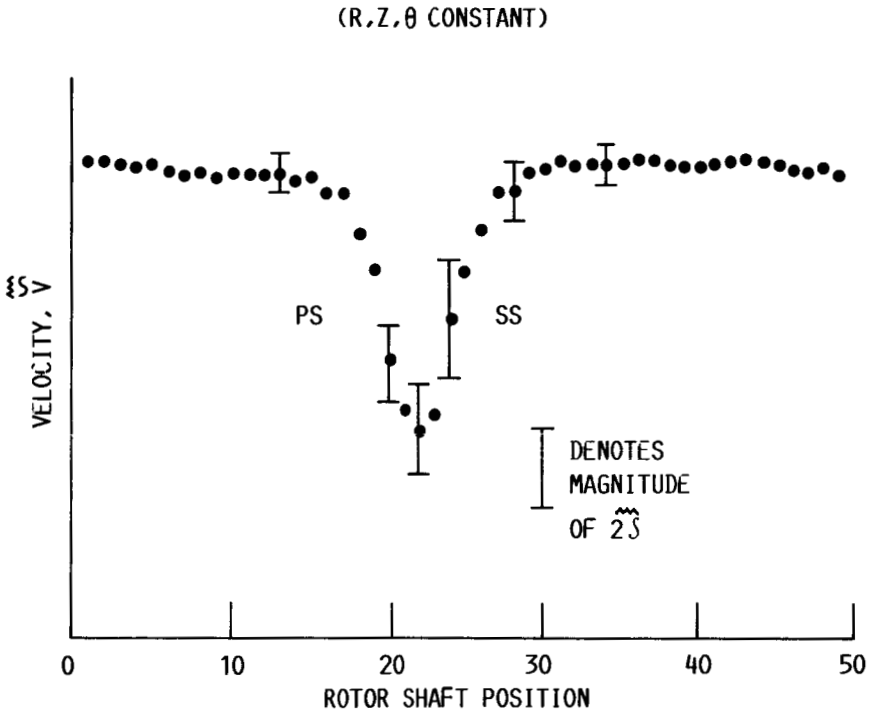

FIGURE 7.- TEMPORALLY PHASE-LOCK AVERAGE VELOCITY DISTRIBUTION REPRESENTING A DESCRIPTION OF THE FLOW FIELD ACROSS A REPRESENTATIVE "AVERAGE" ROTOR PASSAGE.

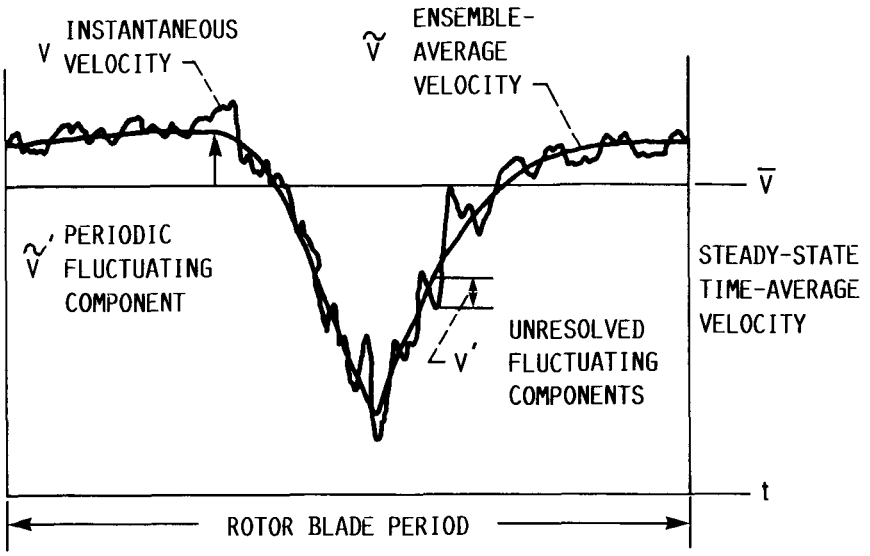

(A) CONTINUOUSLY SAMPLED HOT-WIRE MEASUREMENTS.

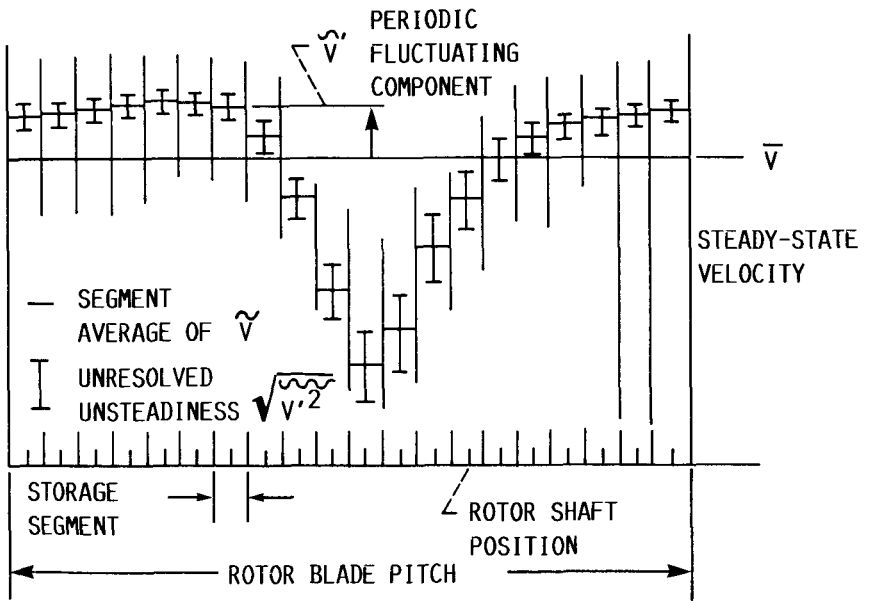

(B) RANDOMLY SAMPLED LFA MEASUREMENTS.

FIGURE 8.- ILLUSTRATION OF THE RELATIONSHIP BETWEEN THE TEMPORAL PHASE-LOCK AVERAGE AND STEADY-STATE VELOCITIES AS WELL AS THEIR RELATIONSHIP WITH ROTOR-WAKE-GENERATED AND UNRESOLVED VELOCITY FLUCTUATIONS FOR BOTH CONTINUOUSLY SAMPLED HOT-WIRE AND RANDOMLY SAMPLED LFA MEASUREMENTS.

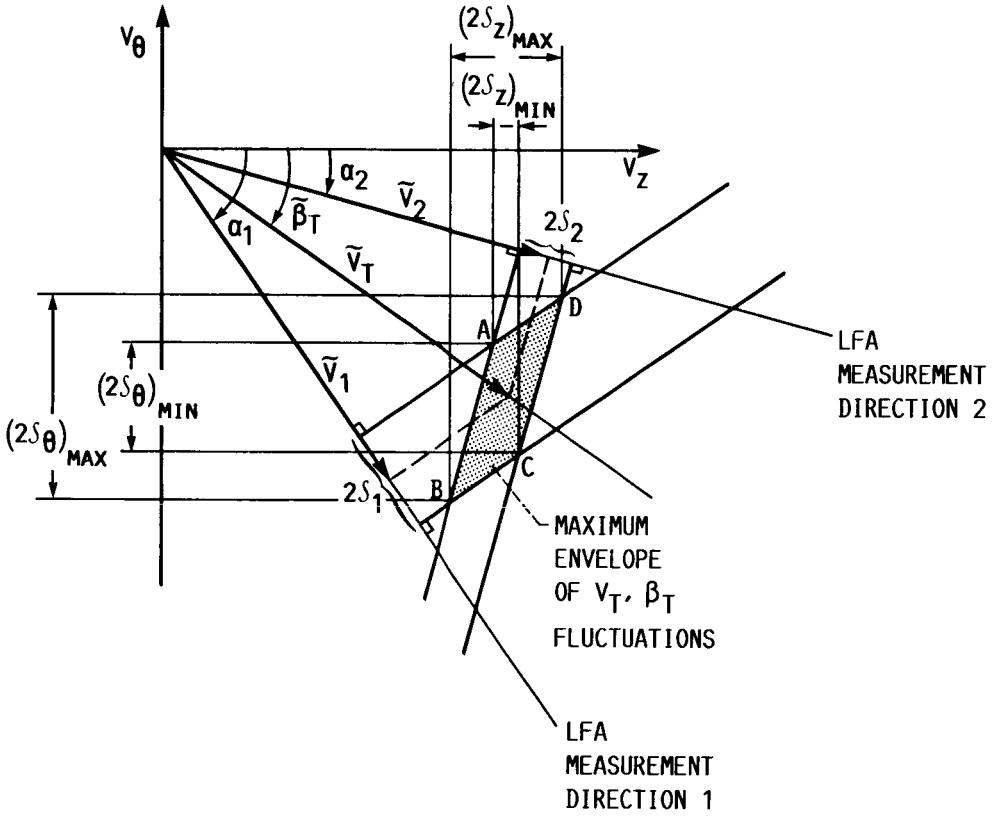

FIGURE 9.- RELATIONSHIP BETWEEN THE ENSEMBLE AVERAGE AND VARIANCES OF THE AXIAL, TANGENTIAL AND MEASURED VELOCITY COMPONENTS, FROM WHICH THE UPPER AND LOWER BOUNDS OF THE UNRESOLVED UNSTEADINESS ARE DETERMINED.

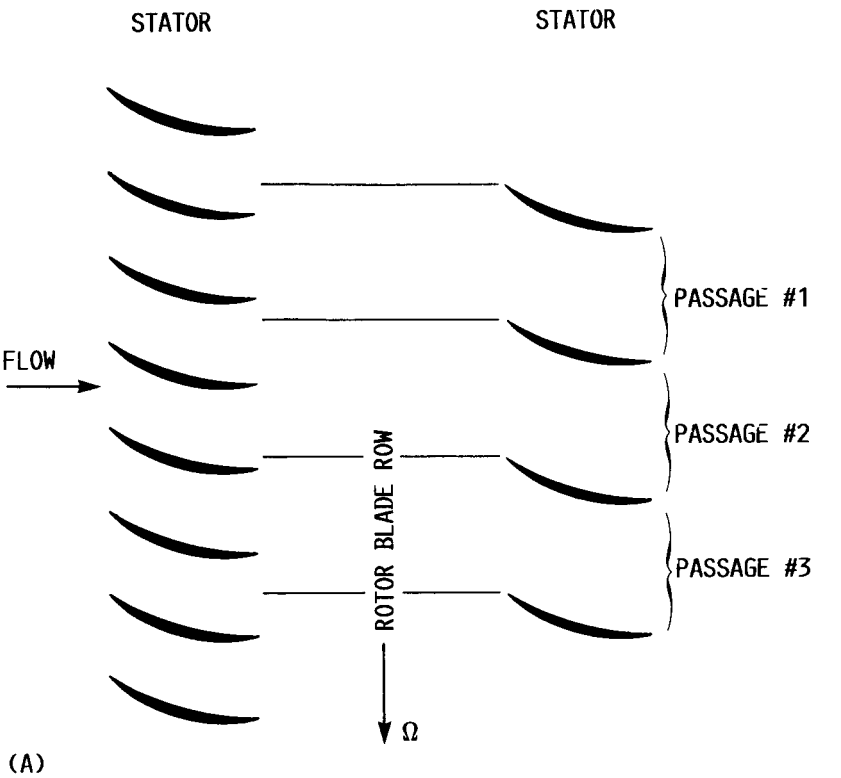

(A)

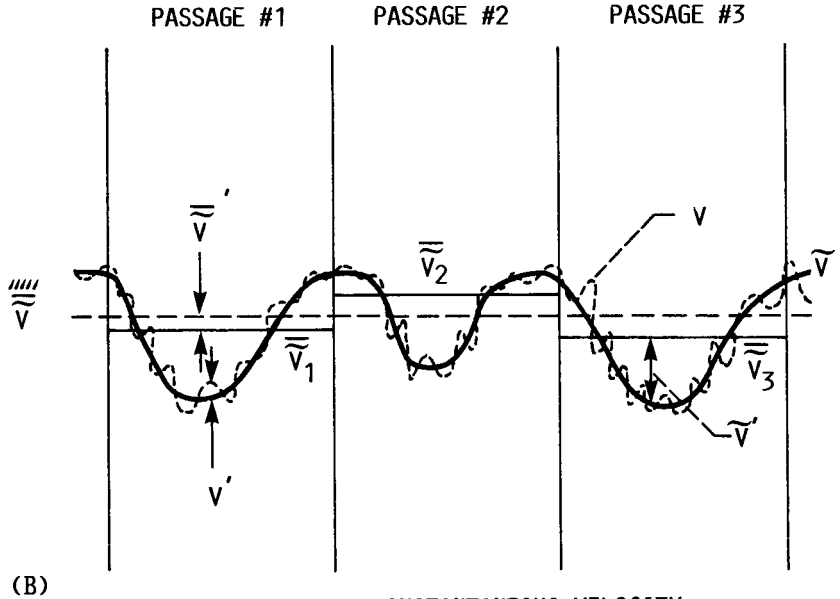

(B)

V = INSTANTANEOUS VELOCITY
$\tilde{V}$ = ENSEMBLE AVERAGED VELOCITY
$\overline{\tilde{V}}$ = STEADY-STATE PASSAGE-TO-PASSAGE AVERAGED VELOCITY

FIGURE 10.- ILLUSTRATION OF THE SPATIALLY APERIODIC FLOWS RESULTING FROM A DIFFERENT NUMBER OF BLADES IN SUCCESSIVE STATOR BLADE ROWS.

1. Report No.	2. Government Accession No.	3. Recipient's Catalog No.
NASA TM-88945 USAAVSCOM-TR-86-C-30		

4. Title and Subtitle	5. Report Date
Measurements of the Unsteady Flow Field Within the Stator Row of a Transonic Axial-Flow Fan I - Measurement and Analysis Technique	
	6. Performing Organization Code 505-62-21
7. Author(s) K.L. Suder, M.D. Hathaway, T.H. Okiishi, A.J. Strazisar, and J.J. Adamczyk	8. Performing Organization Report No. E-3393
	10. Work Unit No.
9. Performing Organization Name and Address NASA Lewis Research Center and Propulsion Directorate, U.S. Army Aviation Research and Technology Activity - AVSCOM, Cleveland, Ohio 44135	11. Contract or Grant No.
	13. Type of Report and Period Covered Technical Memorandum
12. Sponsoring Agency Name and Address National Aeronautics and Space Administration Washington, D.C. 20546 and U.S. Army Aviation Systems Command, St. Louis, Mo. 63120	14. Sponsoring Agency Code

15. Supplementary Notes

Prepared for the 32nd International Gas Turbine Conference and Exhibition sponsored by the American Society of Mechanical Engineers, Anaheim, California, May 31 - June 4, 1987. K.L. Suder, A.J. Strazisar, and J.J. Adamczyk, NASA Lewis Research Center; M.D. Hathaway, Propulsion Directorate, U.S. Army Aviation Research and Technology Activity - AVSCOM; T.H. Okiishi, Iowa State University, Ames, Iowa 50010.

16. Abstract

This two-part paper presents detailed laser anemometer measurements of the unsteady velocity field within the stator row of a transonic axial-flow fan. The objective of this study was to provide additional insight into unsteady blade-row interactions within high speed compressors which affect stage efficiency, energy transfer, and other design considerations. Part I of this paper describes the measurement and analysis techniques used for resolving the unsteady flow field features. The ensemble-average and variance of the measured velocities are used to identify the "rotor-wake-generated" and "unresolved" unsteadiness, respectively. (The term "rotor-wake-generated" unsteadiness refers to the unsteadiness generated by the rotor wake velocity deficit and the term "unresolved" unsteadiness refers to all remaining contributions to unsteadiness such as vortex shedding, turbulence, mass flow fluctuations, etc.). A procedure for calculating auto and cross correlations of the rotor-wake-generated and unresolved unsteady velocity fluctuations is described. These unsteady-velocity correlations have significance since they also result from a decomposition of the Navier-Stokes equations. This decomposition of the Navier-Stokes equations resulting in the velocity correlations used to describe the unsteady velocity field will also be outlined in this paper.

17. Key Words (Suggested by Author(s))	18. Distribution Statement
Unsteady flows; Blade row interactions; Laser anemometry; Compressors; Stator	Unclassified - unlimited STAR Category 02

19. Security Classif. (of this report)	20. Security Classif. (of this page)	21. No. of pages	22. Price*
Unclassified	Unclassified		

*For sale by the National Technical Information Service, Springfield, Virginia 22161